GAO, Dian-ce, et al. A system-level fault detection and diagnosis method for low delta-T syndrome in the complex HVAC systems. Applied energy, 2016, 164: 1028-1038.

https://doi.org/10.1016/j.apenergy.2015.02.025

A System-level Fault Detection and Diagnosis Method for Low Delta-T Syndrome in the Complex HVAC Systems

Dian-ce Gao, Shengwei Wang*, Kui Shan, and Chengchu Yan

Department of Building Services Engineering,
The Hong Kong Polytechnic University, Hong Kong

Abstract:

Low delta-T syndrome widely exists in the existing air-conditioning systems and results in increased energy consumption. This paper presents a system-level fault detection and diagnosis method (FDD) to detect and diagnose the low delta-T syndrome resulted from the performance degradation of AHUs system and plate heat exchanger system in a complex HVAC system. Performance indices are introduced to characterize the health status (normal or faulty) of the system. Reference models are developed to generate the benchmarks of the performance indices under fault-free conditions. In order to mitigate the impact of the model fitting uncertainty of the reference models and the measurement uncertainty of the performance indices, adaptive thresholds are adopted using t-statistic approach to identify the health conditions of the performance indices. The proposed method was validated in a dynamic simulation platform built based on a real complex HVAC system studied. The results show that the proposed FDD strategy can successfully detect the low delta-T syndrome, identify the related faults and quantitatively evaluate of the faults severity.

Keywords: *Chilled water system; low delta-T syndrome; fault detection and diagnosis; adaptive threshold.*

* Corresponding author. +852 27665858; fax: +852 2774 6146.
E-mail address: beswwang@polyu.edu.hk

1. Introduction

Heating ventilating and air-conditioning (HVAC) systems are the major energy consumers in the commercial buildings [1]. Currently, the primary-secondary chilled water systems still dominate in the existing commercial buildings. A typical primary-secondary chilled water distribution system consists of two loops: the primary loop and the secondary loop. In the primary loop, each chiller is associated with a constant speed primary pump to ensure the constant flow through the individual chiller. In the secondary loop, variable speed pumps are employed to achieve variable flow rate according to the cooling demands of the terminal Air-Handling Units (AHUs). The two loops are decoupled by a bypass pipeline. In the high-rise commercial buildings, complex primary-secondary chilled water systems are normally employed, which utilizes multiple plate heat exchangers as the heat transfer station for delivering cooling from low floors to higher levels to avoid extremely high static pressure. Normally, the flow rate of secondary loop should be equal to that of the primary loop under full load condition and should be less than that of primary loop under part load conditions.

However, in practical applications, many primary-secondary chilled water systems do not work as efficiently as expected due to the excessive secondary flow demand, which causes deficit flow problem (i.e. the required flow rate of secondary loop exceeds that of the primary loop). When the deficit flow problem exists, the system water temperature difference (delta-T) produced by the air handling terminals is much lower than the design value, which is known as the low delta-T syndrome [2-4]. The deficit flow problem and low delta-T syndrome may cause a series of operational problems, such as the high supply water temperature to terminal units, the over-supplied chilled water and the increased energy consumption of the secondary pumps. Kirsner [2] pointed out that the low delta-T chilled water plant syndrome exists in almost all large chilled water systems.

The low delta-T syndrome is one of the critical operation problems degrading the building energy performance, which was frequently studied in the last two decades [5-15]. Many possible reasons of the low delta-T syndrome have been studied [6-9]. Taylor [7] summarized some typical causes that causing the low delta-T syndrome. Some causes can be avoided,

such as improper set-point or controls calibration, the use of three-way valves, improper coil and control valve selection, no control valve interlock, and uncontrolled process load, etc. While some causes cannot be avoided, such as reduced coil effectiveness (e.g. fouling), outdoor air economizers and 100% outdoor air systems. Gao [9] presented a case study on diagnosing the low delta-T problem resulted from the deficit flow that frequently occurred in the chilled water system of a super high-rise building. The improper set-point of outlet water temperature on the secondary side of heat exchangers is finally diagnosed as the fault that resulted in the deficit flow and low delta-T syndrome.

Some studies focused on dealing with the low delta-T syndrome and deficit flow problem [10-15]. Among the studies, Fiorino [10] indicated strongly that a higher delta-T could be achieved by proper application of cooling coils, controls systems, distribution pumps, and piping systems. Up to 25 practical methods are recommended to achieve high chilled water delta-T ranging covering component selection, sensor calibration, and configurations of distribution systems, etc. Gao [15] presented a fault-tolerant control strategy for secondary chilled water pump systems to mitigate the low delta-T problem. The strategy modulates the speed of the secondary pumps to ensure the water flow of secondary loop not exceed that of the primary loop while still maintaining highest possible delivery capacity of cooling to terminals. Kirsner [4] analyzed the advantage the use of check valve in the bypass line and thought that installing check valve in the bypass line is a cheap and a simple improvement to primary-secondary design of chilled water plants that allows a plant to deal with low delta-T syndrome. Wang [12] presented an approach that experimentally validated the feasibility of using a check valve in the chilled water bypass line to solve the low delta-T syndrome. Results showed that about 9.2% of total energy consumption of the chillers and secondary water pumps was saved in the test case when compared with the case when no check valve used.

The existing studies demonstrate that low delta-T syndrome widely existed in the primary-secondary chilled water system and the elimination of this problem can improve the energy efficiency of the chilled water system. Therefore, the delta-T of the overall system is an essential indicator that indicates the healthy status of the entire chilled water system.

Lower system temperature difference means excessive chilled water is delivered and more energy is wasted. It is very important to monitor and diagnose whether or not the system temperature difference is in normal conditions and to what extent it deviates from the normal values. However, some challenges have to be addressed when diagnosing the system temperature difference. The system temperature difference is an average value of the differential temperatures produced by individual AHUs. The system temperature difference will vary with the changing of total cooling load and each AHU's load. Because there are no enough sensors (e.g. water flow rate, return water temperature) for individual AHUs in most of the existing HVAC systems, there would be difficult to diagnose the temperature difference of each AHU separately. Actually, in real applications, a slightly lower system delta-T is hard to be identified by the operators until it is worsened to be highly lower than the normal value (e.g. delta-T is 2-3 °C) after a long time. Therefore, it is necessary to detect and identify the lowered temperature difference as soon as possible so that less energy can be wasted. It is also import to find the causes that result in the lowered temperature difference.

Among the possible causes, the reduced effectiveness of cooling coils or/and heat exchangers is one of the major causes, which inevitably occurs after a long operating time. For instance, when the performance of the cooling coil is degraded, such as coil fouling, the heat transfer effect between the inlet air and inlet water is significantly decreased. More chilled water is required and the water temperature difference produced by the coil is decreased when handling the same cooling load. Some existing studies have paid efforts on the diagnosis of the fouling in coils and heat exchangers [16-19].

Unlike the existing studies focusing on the diagnosis of fouling in individual cooling coils or heat exchangers, this study therefore provides a system-level fault detection and diagnosis (FDD) method for detecting and quantitatively diagnosing the low delta-T syndrome in the complex HVAC system involving plate heat exchangers. This system-level FDD method pays more attention to the healthy status of the water temperature difference of the AHUs system and plate heat exchanger system as a whole, respectively. The temperature differences of both the AHUs system and heat exchanger system will be detected and evaluated quantitatively. Performance indices are also developed to identify the faults concerning the degraded AHUs

and plate heat exchangers, which are the two main causes for the low delta-T syndrome.

Three major innovative works are involved in this study. First, the proposed method is based on the system-level, which is cost-effective and needs a small amount of measurement sensors when compared to the component-level method. Second, load ratios of individual AHUs are introduced as the drive variables to enhance the prediction accuracy of reference models for the water temperature difference of AHUs system, which considers the time-varying load distribution of individual AHUs with high nonlinearity. Third, adaptive thresholds are introduced to enhance the detection ratio using the t-statistic approach for mitigating the uncertainties from the measurements and model fittings. This method is evaluated on a simulated dynamic system constructed based on a real system in a high-rise building in Hong Kong.

Since the primary constant-secondary variable chilled water systems are still the typical configurations in the existing building HVAC systems, the FDD method presented in this paper is developed and customized based on a high rise building in Hong Kong. Therefore, this paper firstly introduces the case study building and then the method proposed. This paper is organized as follows: Section 2 gives a brief description of the studied building and HVAC system. The formulation of the FDD strategy is then introduced in Section 3. Section 4 describes the FDD method validation and discussion. The last section is the conclusion.

2. Building and system description

The central cooling system concerned in this study is a complex primary-secondary chilled water system in a super high-rise building in Hong Kong [20]. The building is about 490 meters high with approximately 321,000 m^2 floor areas, consisting of a basement of four floors, a block building of six floors and a tower building of 98 floors. As shown in Fig. 1, this central chilled water plant employs six identical constant speed centrifugal chillers to provide chilled water for air handling units in the building. The rated cooling capacity and power consumption of each chiller are 7230 kW and 1270 kW respectively. The design chilled water supply and return temperatures for chillers are 5.5°C and 10.5°C respectively. Each chiller is associated with a constant speed primary chilled water pump. The primary

loop is decoupled with the secondary loop through the bypass line. The secondary chilled water system is divided into four zones, in which Zone 2 is supplied with the chilled water from chillers directly. The plate heat exchangers are employed to transfer cooling energy from chillers to terminal air-handling units in Zone 1, Zone 3 and Zone 4 to avoid chilled water pipelines and terminal units from suffering extremely high static pressure. All the secondary pumps are equipped with variable speed drivers and all the primary pumps are constant speed pumps. The specifications of chilled water pumps are listed in Table 1. This central chilled water plant frequently suffered from the deficit flow problem and low delta-T syndrome after its use since the middle of 2008 [9].

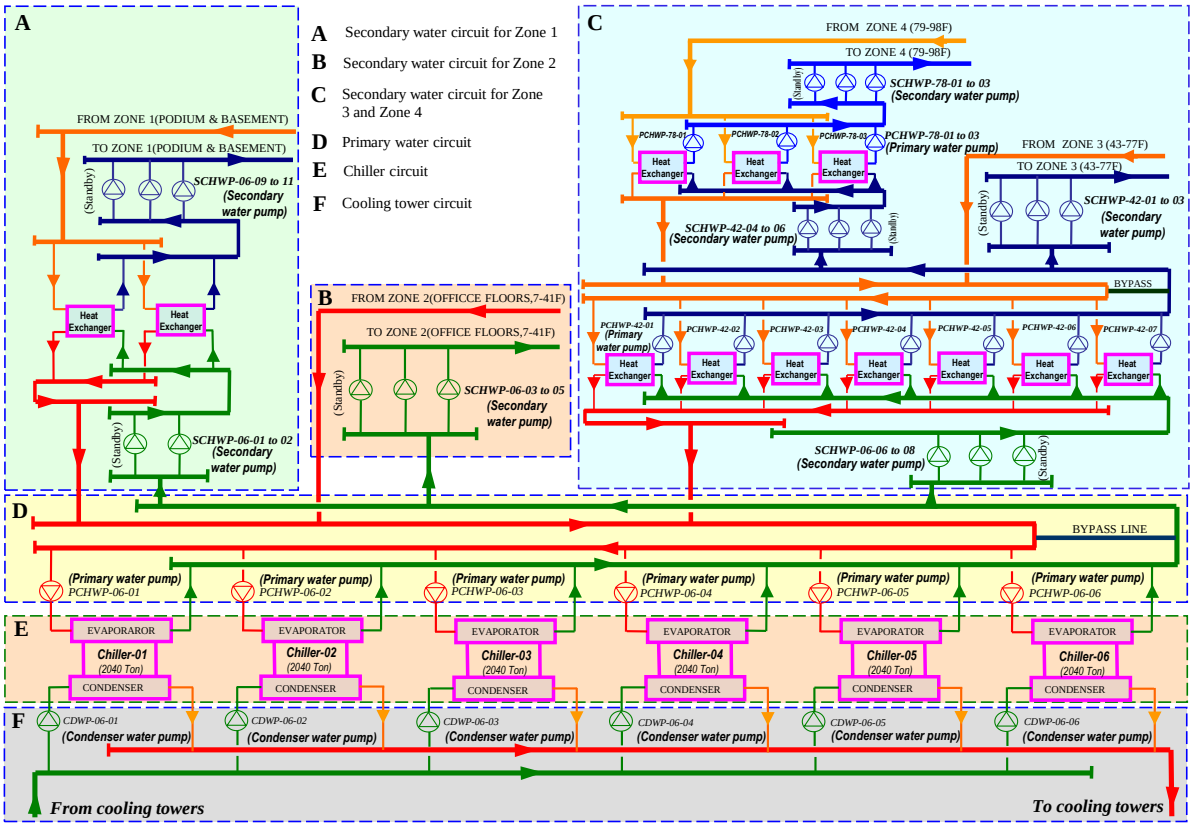

Fig. 1 Schematic of the chilled water system

The subsystem of Zone 3 is selected as the example to be studied due to that it is the complicated primary-secondary system involving plate heat exchangers. Such pumping paradigm is normally adopted in the chilled water distribution system in most of actual high-rise buildings. The simplified schematic of Zone 3 is illustrated in Fig. 2. In this subsystem studied, plate heat exchangers are employed to transfer the cooling energy from the chiller to the terminal AHUs. At the primary side of heat exchangers (i.e., before heat

exchangers), variable speed pumps (SCHWP-06-06 to 08) deliver the chilled water from the chillers to the plate heat exchangers. At the secondary side of heat exchangers (i.e., after heat exchangers), each plate heat exchanger is associated with a constant speed pump to ensure the constant flow rate at the secondary side of each heat exchanger. Variable speed pumps (SCHWP-42-01 to 03) are employed to deliver the outlet water from the heat exchangers to the terminal AHUs.

Table 1 Specifications of chilled water pumps

Pumps	Number*	Flow (*L/s*)	Head (*kPa*)	Power (*kW*)	Remarks
Primary water pumps					
PCHWP-06-01 to 06	6	345	310	126	Constant speed
Secondary pumps for Zone1					
SCHWP-06-01 to 02	1(1)	345	241	101	Variable speed
SCHWP-06-09 to 11	2(1)	155	391	76.9	Variable speed
Secondary pumps for Zone 2					
SCHWP-06-03 to 05	2(1)	345	406	163	Variable speed
Pumps for Zone 3 and Zone 4					
SCHWP-06-06 to 08	2(1)	345	297	122	Variable speed
PCHWP-42-01 to 07	7	149	255	44.7	Constant speed
SCHWP-42-01 to 03	2(1)	294	358	120	Variable speed
SCHWP-42-04 to 06	2(1)	227	257	69.1	Variable speed
PCHWP-78-01 to 03	3	151	202	36.1	Constant speed
SCHWP-78-01 to 03	2(1)	227	384	102	Variable speed

*Value in parentheses indicates number of stand by pumps

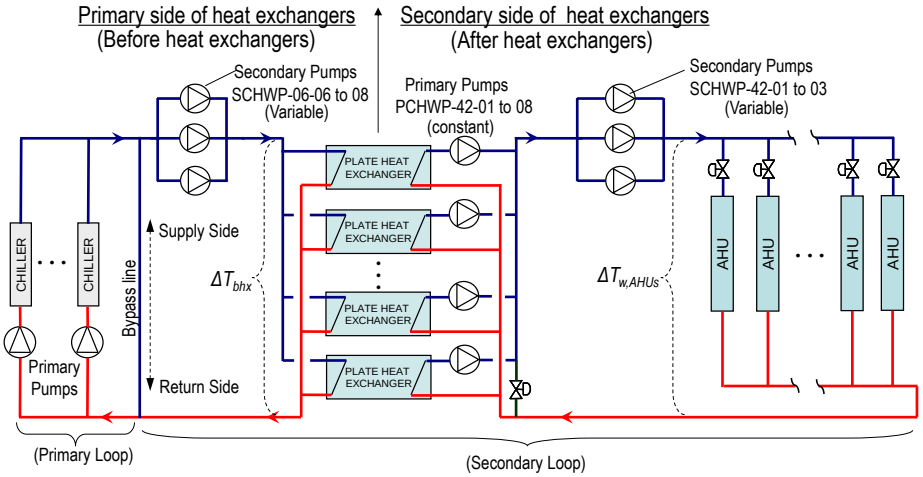

Fig. 2 The simplified schematic of chilled water system of Zone 3

3. Formulation of the FDD method

3.1 Outline of the method

The FDD strategy for diagnosing the low delta-T syndrome, as shown in Fig. 3, mainly includes two sections: an online FDD process and an offline model training process.

In the online FDD process, the data measured from HVAC system are firstly preprocessed to remove the obviously unreasonable and dynamical data through outlier removing and data filter. At the fault detection stage, performance indices (PIs) are calculated using the filtered measured data to characterize the current healthy status of the system. Reference models are developed to determine the benchmarks of the PIs. Regression models are adopted to develop the reference models of the PIs concerning the performance of AHUs system and plate heat exchanger system. Then, the residuals between the calculated PIs and the corresponding benchmarks are compared with their online adaptive thresholds to detect whether or not the faults occur. When the residual of one PI is located out of its threshold band, the corresponding PI are considered to be in the abnormal condition. The adaptive thresholds of PIs are calculated using the t-statistic approach in order to mitigate the impact of measurement and modeling uncertainties. The thresholds can be updated online according to the time-varying operating conditions. At the fault diagnosis stage, the fault with the abnormal PI is identified and the severity is assessed quantitatively.

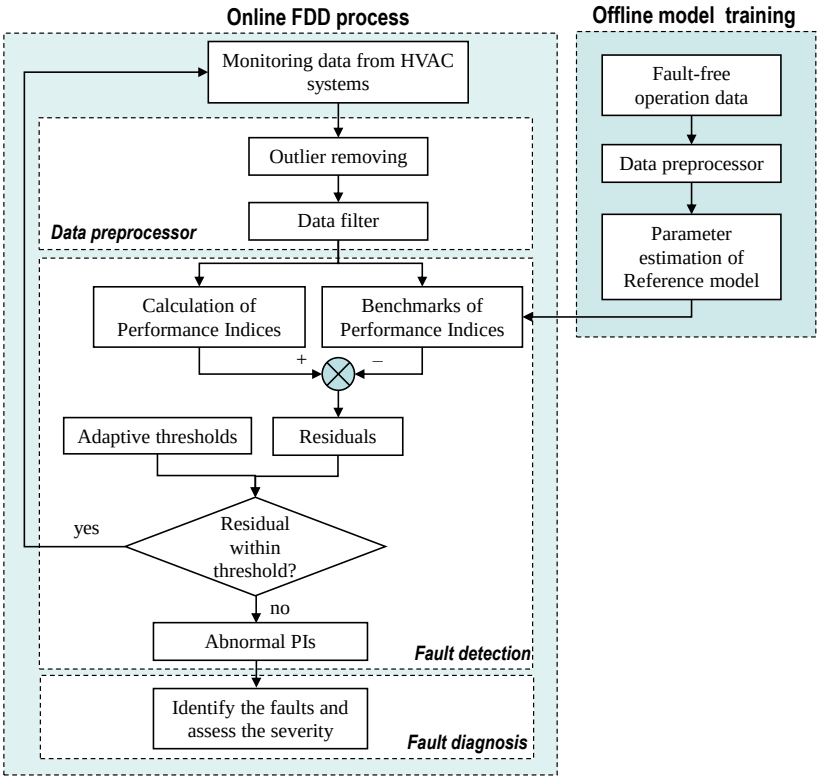

Fig. 3 Schematic of the FDD strategy

In the offline model training section, the historical operation data without faults are used as

the sampling data to train the reference models. The fault-free operating data covering a wide range of operating conditions is selected to ensure the high detection ratio of faults.

The detailed descriptions of the FDD strategy are presented in the followings sections.

3.2 Faults modeling using performance indices

In the studied complex system as described in Fig. 2, two sub-systems, the AHUs system and the plate heat exchanger system, are diagnosed because their performance degradations could result in the lowered system delta-T and increased energy consumption of chilled water pumps.

Table 2 Faults, fault modeling and PI formulations

Fault	Means of introducing faults	Performance indices(PIs)	PIs formulation	Variation trend
Performance degradation in the sub-system of AHUs	Increase thermal resistance at water side	Water temperature difference of overall AHUs	$\Delta T_{w,AHUs}=T_{w,out,AHU}-T_{w,in,AHU}$	$\Delta T_{w,AHUs}\downarrow$
		Overall conductance–area product	$UA_{AHUs}=Q_{tot,AHUs}/LMTD$	$UA_{AHUs}\downarrow$
Performance degradation in the sub-system of plate Heat exchangers	Decrease the heat transfer coefficient	Water temperature difference of the system	$\Delta T_{w,bhx}=T_{w,out,bhx}-T_{w,in,bhx}$	$\Delta T_{w,bhx}\downarrow$
		Overall conductance–area product	$UA_{HX}=Q_{tot,HX}/LMTD$	$UA_{HX}\downarrow$

Performance indices (PIs) are proposed to characterize the healthy status of different sub-systems respectively. Table 2 presents the faults and the corresponding means of introducing faults as well as the proposed PIs. Faults are introduced by tuning the parameters of the dynamic models on the simulation platform built according to Fig. 2. Two severity levels for each fault are investigated in this study. Different severity levels of faults are introduced by changing quantities of the related parameters. It is noted that the means of introducing faults used in this study are just one alternative way for demonstrative case studies. Detailed descriptions of faults introduction and the relationship between the faults and the corresponding PIs are interpreted as follows:

1) Performance degradation of the sub-system of AHUs. The sub-system involving multiple AHUs is considered as a whole to be studied. Two PIs are selected to identify the performance degradation of AHUs system: the water temperature difference ($\Delta T_{w,AHUs}$) produced by all AHU cooling coils of the sub-system and the overall conductance–area

product (UA_{AHUs}) of all AHUs. When the performance of the overall AHUs system are degraded, the heat transfer capacity between the inlet air and the inlet chilled water will be reduced. For the given total cooling load ($Q_{tot,AHUs}$) of the sub-system, more chilled water is required to handle the same amounts of cooling load, causing a lowered water temperature difference (ΔT_{AHUs}) produced by all the AHUs. In order to simulate the performance degradation of AHUs system, thermal resistance at water side for each AHU is artificially increased by two levels respectively (i.e., water thermal resistance is increased by 20% and 40%).

2) Performance degradation of the sub-system of plate heat exchangers. The sub-system involving multiple plate heat exchangers is considered as a whole to be studied. Two PIs are selected to identify the performance degradation of heat exchanger system: the water temperature difference ($\Delta T_{w,bhx}$) produced at the primary side of heat exchanger group (i.e., before heat exchangers) and the overall conductance–area product (UA_{HX}) of the heat exchanger group. Plate heat exchangers are employed as heat transfer stations for delivering cooling from chillers to the AHUs at higher floors in high-rise buildings. When UA_{HX} is reduced, more chilled water is required before heat exchangers to transfer the same cooling energy for lowering down the water temperature at the secondary side of heat exchanger group (i.e., after heat exchangers). Consequently, the water temperature difference before heat exchangers ($\Delta T_{w,bhx}$) is reduced. The performance degradation of heat exchangers is simulated by reducing the heat transfer coefficient of individual plate heat exchanger artificially in two quantities (i.e., UA_{HX} is reduced by 20% and 40%) in the simulation platform.

3.3 Reference models of performance indices

Reference models are developed to determine the benchmarks of the proposed PIs.

3.3.1 AHU system

The studied AHUs system is a variable air volume (VAV) system. For each AHU, the supply air temperature is controlled at the preset set-point by modulating the required chilled water flow rate. For the individual AHU, the chilled water temperature difference produced is

strongly dependent on the cooling load of this AHU, the inlet water temperature and the inlet air temperature. However, for a system involving multiple AHUs, the water temperature difference ($\Delta T_{w,AHUs}$) produced by the overall system would be complex. $\Delta T_{w,AHUs}$ is not only dependent on the total cooling load of the system, the inlet water/air temperatures, but also affected by the cooling load ratios of individual AHUs. It means that although the total cooling load handled by the overall AHUs is the same, the average temperature difference of the system water would be significantly different if cooling load ratios of individual AHUs are different.

For instance, a simulation-based case study was conducted to study the variation of the average water temperature difference (delta-T) of a system consisting of two identical AHUs. In the study, the total cooling load handled by the two AHUs was maintained unchanged at all time, and only the cooling load ratios of the individual AHUs varied. In the simulations, the temperature and humidity of the inlet air as well as the inlet water temperature were fixed, and the water flow rate of the coil was modulated to control the outlet air temperature at a fixed set-point. From the results shown in Table 3, when the cooling load of each AHU is the same (Case #1), the system water delta-T is 6.49 °C. When the cooling load ratio of AHU-1 is 0% and the cooling load ratio of AHU-2 is 100% (Case #6), the average system water delta-T is 5.08 °C, which is 20.9% lower than that in Case #1. The test results indicate that the load ratios of individual AHUs are the sensitive variables that affect the average delta-T of the entire AHUs system.

Table 3 System temperature difference under various cooling load distributions

Cases	AHU-1		AHU-2		Total		Deviation of system Delta-T (%)
	Individual Delta-T (°C)	Individual load Ratio (%)	Individual Delta-T (°C)	Individual load Ratio (%)	System Delta-T (°C)	System load Ratio (%)	
Case #1 (Benchmark)	6.49	50	6.49	50	6.49	50	-
Case #2	6.81	40	6.19	60	6.42	50	-1.1
Case #3	7.07	30	5.90	70	6.20	50	-4.5
Case #4	7.19	20	5.62	80	5.87	50	-9.6
Case #5	6.55	10	5.35	90	5.44	50	-16.2
Case #6	0	0	5.08	100	5.08	50	-20.9

When studying the performance of AHUs group as a whole, the cooling ratios of individual AHUs were not properly considered in the existing studies [21, 22]. In this study, the reference model of system temperature difference ($\Delta T_{w,AHUs}$) of AHUs system can be developed shown in Eq.(1), in which the cooling load ratios of individual AHUs (i.e., Rat_1... Rat_n) are considered as the important influence factors. In order to determine the load ratio of each AHU, installation of an energy meter for each AHU would be a good choice. However, there is normally no energy meter (or water flow meter) installed for the individual AHUs in most of real HVAC systems due to the initial cost. To address this issue, the measured air flow rate (Ma) of each AHU fan divided by the design value (Ma_{des}) can be employed to indicate the load ratio approximately, as shown in Eq.(2). The air flow rate can be easily determined by the simple air flow measurement instrument like the pitot tube.

Since the overall conductance–area product (UA_{AHUs}) is not so sensitive to the load ratios of individual AHUs under the situation when the inlet water/air temperatures maintains stable, the reference model of UA_{AHUs} is developed shown in Eq.(3).

$$\Delta T_{w,AHUs} = a_0 Q_{AHUs}^{a_1} T_{w,in,AHUs}^{a_2} T_{a,in,AHUs}^{a_3} \prod_{i=1}^{n} Rat_i^{g_i} \quad (1)$$

$$Rat_i = Ma(i) / Ma_{des}(i) \quad (2)$$

$$UA_{AHUs} = b_0 Q_{AHUs}^{b_1} T_{w,in,AHUs}^{b_2} T_{a,in,AHUs}^{b_3} \quad (3)$$

where, Q_{AHUs} is the total cooling load of the AHUs group. $T_{w,in\ ,AHUs}$ is the inlet water temperature of AHUs. $T_{a,in\ ,AHUs}$ is the average inlet air temperature of all the AHUs. Rat_i is the load ratio of the ith AHU. n is the number of AHUs in operation. $Ma(i)$ is the measured air flow rate of the ith AHU fan, $Ma_{des}(i)$ is the design air flow rate of the ith AHU. The coefficients (i.e., a_0–a_3, b_0–b_3, g_i) are constant, which can be determined by the least square method using the fault-free operation data obtained from the building automation (BA) system.

3.3.2 Plate heat exchanger system

Compared to the AHUs system, the plate heat exchanger system is not so complex due to the fact that all the heat exchangers in the group are the same type/capacity and water through

each active heat exchanger is approximately equal. Simplified regression models are developed by selecting the driving variables as the regressors.

The cooling load (Q_{HX}) of the entire heat exchanger group, the inlet water temperature at the primary and secondary sides of heat exchangers ($T_{w,in,bhx}$ and $T_{w,in,ahx}$), and the total water flow rates at primary and secondary sides of heat exchanger group ($M_{w,in,bhx}$ and $M_{w,in,ahx}$) are selected as the driving variables to form the reference model of the temperature difference of water at primary side of heat exchangers ($\Delta T_{w,bhx}$), as shown in Eq. (4). Since the overall conductance–area product (UA_{HX}) of heat exchangers is highly dependent on the water flow rates at both the primary and secondary sides of heat exchangers, Eq. (5) is used as the reference model of UA_{HX}.

$$\Delta T_{w,bhx} = c_0 \cdot Q_{HX}^{c_1} \cdot T_{w,in,bhx}^{c_2} \cdot T_{w,in,ahx}^{c_3} \cdot M_{w,bhx}^{c_4} \cdot M_{w,ahx}^{c_5} \quad (4)$$

$$UA_{HX} = d_0 \cdot M_{w,bhx}^{d1} \cdot M_{w,ahx}^{d2} \quad (5)$$

The coefficients (i.e., c_0–c_5, d_0–d_2) used in the two reference models are constant, which can be determined off-line by the least square method using the related fault-free operating data.

3.3.3 Fault detection using adaptive thresholds

At every time step, the performance indices (PIs) and their benchmarks are calculated using the related measured operating data respectively. A residual of each PI can be generated when comparing the PI with its benchmark. The residual threshold is used to determine whether the PI is in abnormal condition. When the residual of one PI is beyond its threshold, it means this PI is in the abnormal condition. Therefore, the accuracy of the residual threshold has significant effect on the fault detection rates.

However, there are significant uncertainties in the calculation processes of both PIs and their benchmarks. The uncertainty of the PI comes from the measurement uncertainty due to the accuracy of sensors. The uncertainty of the benchmark is subject to the model fitting errors from the reference models. Particularly, the design temperature difference of the overall AHUs is a small value (e.g. 5°C). A deviation of plus-minus 0.5°C would result in the error of 20%.

In this study, statistical methods are used to generate the adaptive thresholds that vary with operating conditions when given certain confidence levels. Because the residual of each PI and the related reference model are variables depending on the operating conditions, the threshold of each PI residual is supposed to be a variable varying according to different operating conditions. The method to determine the adaptive thresholds are based on the study of Cui [23] using t-statistic approach, which can be briefly introduced as below.

Under a certain confidence level, the threshold of PI residuals can be determined by Eq. (5).

$$Thr_i = U(\tilde{r}_i) = t_{\alpha/2,n-p}\tilde{\sigma}_{\tilde{r}_i - r_i} \tag{5}$$

Where, Thr_i is the threshold of the residual of the ith performance index residual, $U(\tilde{r}_i)$ is the uncertainty of the residual at a certain confidence level, $\tilde{r}_i$ is the estimator of the residual of the ith performance index, r_i is the true value of the residual of the ith performance index, $\tilde{\sigma}^2_{\tilde{r}_i - r}$ is the estimated variance of $\tilde{r}_i - r_i$, $t_{\alpha/2,n-p}$ is the value of the t distribution with n-p degrees of freedom at a confidence level of (1-α), n is the number of training data points used in the model regression and p is the number of coefficients estimated from the training data.

The true value of the residual (r_i) can be expressed shown in Eq. (6) and the estimator of the residual, $\tilde{r}_i$, can be describe as shown in Eq.(7).

$$r_i = g_i(z) - Y_i \tag{6}$$

$$\tilde{r}_i = g_i(\hat{z}) - \tilde{Y}_i \tag{7}$$

Where, $g_i(\cdot)$ is the formula of the ith performance index presented in Table 1, $\mathbf{z}$ is the vector of the true values of the variables included in $g_i(\cdot)$, $\hat{z}$ is the vector of the measured values of the variables included in $g_i(\cdot)$, Y_i is observed value of the ith performance index corresponding to a specific observed regressor vector ($\hat{\boldsymbol{V}}$), which can be given in Eq.(8). $\tilde{Y}_i$ is the output of the ith reference model corresponding to the same observed regressor vector ($\hat{\boldsymbol{V}}$).

$$Y_i = f_i(\hat{V}) + \gamma_i \tag{8}$$

where, $f_i(\cdot)$ is the proposed formula of the reference model of the ith performance index, γ_i is normally distributed error with a mean of zero and a variance of the regression error of Y_i, $\hat{\boldsymbol{V}}$

is the vector of the measured values of the variables included in $f_i(\cdot)$.

The estimated variance ($\tilde{\sigma}^2_{\tilde{r}_i - r}$) of $\tilde{r}_i - r_i$ is determined by Eq. (9).

$$\tilde{\sigma}^2_{\tilde{r}_i - r_i} = \sum_j \left[\left(\frac{\partial g_i}{\partial z_j} \right) \sigma_{z_j} \right]^2 + \tilde{\sigma}^2_{Y_i} [1 + \mathbf{X}_0^T (\mathbf{X}_{reg}^T \mathbf{X}_{reg}) \mathbf{X}_0] \quad (9)$$

where, g_i is the formula for calculating the ith performance index. z_j is the jth element in the vector of measured variables (**z**), which is used to calculate the ith performance index. σ_{z_j} is the standard deviations of z_j and $\tilde{\sigma}^2_{Y_i}$ is the estimated variance of the regression error of ith performance index(Y_i). $\mathbf{X}_0$ is the vector of regressor for the current prediction and $\mathbf{X}_0^T$ is the transpose of $\mathbf{X}_0$. $\mathbf{X}_{reg}$ is the matrix of regressor associated with the training data and $\mathbf{X}_{reg}^T$ is the transpose of $\mathbf{X}_{reg}$.

It is worth pointing out that the first part at the right side of Eq. (9) indicates the measurement uncertainty associated with the accuracy of sensors and the second part at the right side of Eq.(9) indicates the uncertainty associated with the model fitting errors from the reference models.

3.3.4 Fault severity evaluation

When a performance index is identified to be abnormal, the fault severity can be evaluated to show to what extent the performance index deviates from the normal value. In this study, a coefficient *Dev* is defined as shown in Eq. (10) to quantitatively evaluate the severity level of the performance index suffered from faults. Also, this coefficient is calculated considering the uncertainties of measurement and model fitting by introducing the adaptive threshold of the corresponding performance index.

$$Dev_i = \begin{cases} g_i(\hat{z}) - f_i(\hat{V}) - |Thr_i|, & \text{when } g_i(\hat{z}) - f_i(\hat{V}) > |Thr_i| \\ g_i(\hat{z}) - f_i(\hat{V}) + |Thr_i|, & \text{when } g_i(\hat{z}) - f_i(\hat{V}) < -|Thr_i| \\ 0, & \text{the rest} \end{cases} \quad (10)$$

where, Thr_i is the threshold of the residual of the ith performance index residual, $g_i(\cdot)$ is the formula for calculating the ith performance index. $f_i(\cdot)$ is the formula of the proposed

reference model of the ith performance index, $\hat{z}$ is the vector of the measured values of the variables included in $g_i(\cdot)$, $\hat{\boldsymbol{V}}$ is the vector of the measured values of the variables included in $f_i(\cdot)$.

4. FDD strategy validation and discussions

4.1 Setup of the test platform

Since the studied building is a new-built building, there is no enough sampling data that involve faults for validating the proposed FDD strategy. A dynamic simulation platform was built using the information of the real HVAC system in the studied high-rise building. Detailed dynamic physical models of components (e.g. chiller, cooling coil, plate heat exchanger, and pump) are adopted to simulate the dynamic process of the overall HVAC system. The dynamic simulation platform was used to generate operating data for the validations of the FDD strategy.

The dynamic simulation platform was built based on the simplified HVAC system shown in Fig. 2. This is a typical primary-secondary chilled water system. Two water cooled centrifugal chillers are used to generate the chilled water of 5.5°C under design condition. Each chiller is associated with a constant speed primary pump. In the secondary loop, heat exchangers are used to transfer the cooling energy from the chillers to the terminal units. After each heat exchanger, a primary constant speed pump is installed to ensure the constant flow through each heat exchanger. All the secondary pumps are equipped with VFDs. The AHU valves are modulated to maintain the supply air temperature at its set-point (i.e. 13°C). The AHU fans are also equipped with VFDs to vary supply air flow rate and the VAV boxes are modulated to maintain the indoor air temperature at a fixed set-point (i.e. 23°C). The entire simulation platform is developed using TRNSYS 16. The weather data used is the data of the typical year in Hong Kong. The key dynamic physical models of AHU coils and plate heat exchangers are described briefly as follows.

4.1.1 Dynamic AHU Coil model

The AHU coil model simulates the outlet water and outlet air states. In this study, the physical model developed by Wang [24] is used. The AHU coil is modeled using a dynamic approach. A first-order differential equation, as shown in Eq. (11), is used to represent the dynamics of a coil with lumped thermal mass. The dynamic equation based on the energy balance ensures that the energy is conserved. The outlet air and water temperatures ($t_{a,out}$, $t_{w,out}$) are computed using Eq. (12) and (13) respectively, by the heat balances of both sides. The heat transfer calculation applies the classical number of transfer units (*NTU*) and heat transfer effectiveness methods. The classical method to calculate the effect of the fins in the air side on the thermal resistance is used.

$$C_c \frac{dt_c}{d\tau} = \frac{t_{a,in} - t_c}{R_1} - \frac{t_c - t_{w,in}}{R_2} \tag{11}$$

$$t_{a,out} = t_{a,in} - \frac{SHR\left(t_{a,in} - t_c\right)}{R_1 C_a} \tag{12}$$

$$t_{w,out} = t_{w,in} - \frac{t_c - t_{w,in}}{R_2 C_w} \tag{13}$$

Where, t_c is the mean temperature of the coil, $t_{a,in}$ and $t_{w,in}$ are the inlet air and water temperatures, C_c is the overall thermal capacity of the coil, C_a and C_w are the capacity flow rates of air and water, R_1 and R_2 are the overall heat transfer resistances at air and water sides, *SHR* is the sensible heat ratio.

4.1.2 Dynamic heat exchanger model

The dynamic performance of a heat exchanger is represented by a classical steady-state heat transfer model and a simple dynamic model [24]. The heat transfer model computes the number of transfer units and heat transfer efficiency (ε) using Eq. (14) for a counter flow heat exchanger and Eq. (15) for a crossover flow heat exchanger. Eq. (16) is used to represent the thermal storage characteristics of the heat exchanger and then to simulate its dynamic response.

$$\varepsilon = \frac{1 - \exp\left[-NTU(1-\omega)\right]}{1 - \omega\exp\left[-NTU(1-\omega)\right]} \tag{14}$$

$$\varepsilon = \frac{1 - \exp\left[-\omega(1 - \exp(NTU))\right]}{\omega} \tag{15}$$

Where, ω is the capacity flow rate ratio, ε is the number of transfer units and heat transfer efficiency, and *NTU* is the number of transfer units.

$$C_{hx}\frac{dT'_{hx,in}}{d\tau}=c_{p,w}M_{w,hx}(T_{hx,in}-T'_{hx,in}) \quad (16)$$

Where, T is the origin temperature, T' is the temperature after introducing dynamic effects, $c_{p,w}$ is the specific heat of water, C_{hx} is the overall thermal capacity of the heat exchanger, and the subscript *in,w,hx* indicate inlet, water and heat exchanger, respectively.

4.2 Validation of the FDD strategy

4.2.1 Validation of reference models

The accuracy of the reference models is essential for the FDD strategy. The reference models developed in this study were trained using the fault-free operation data under various operating conditions. The reference model of the delta-T ($\Delta T_{w,AHUs}$) of the global AHUs was trained using the operating data under different system cooling load ratios (between 20% and 100% with step of 10%). Under one certain cooling load, different combinations of AHUs with different load ratios were tested. Since the test results are similar, only the results of the test case with 50% of the system load ratio are shown in Fig. 4(a). For the validation of the other reference models of the performance indices (i.e., UA_{AHUs}, $\Delta T_{w,bhx}$, UA_{HX}), the test cases covering the overall load range of each sub-system between 20% and 100% are conducted and shown in Fig. 4(b), Fig.5(a) and 5(b), respectively.

The “measured” results mean that the PI is calculated by the equations in Table 2 using the measured data. The predicted results mean the predictive values of the PI by the reference models. It can be seen that most of the predicted values agreed well with the “measured” ones, which indicates that the reference models have good performances in prediction.

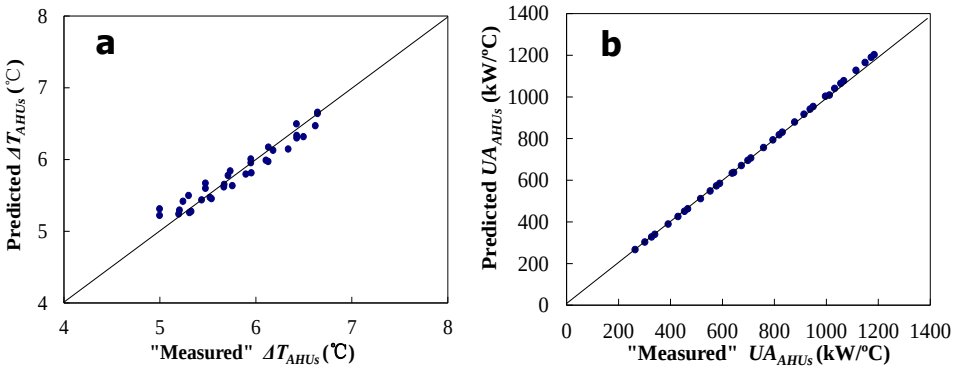

Fig. 4 Validation results of the reference models for AHUs system

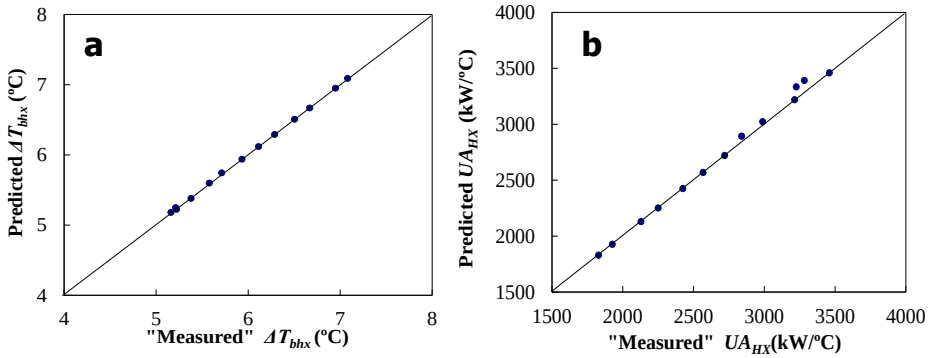

Fig.5 Validation results of the reference models for heat exchangers system

4.2.2 Validation of the FDD strategy

Three typical days (8:00am to 18:00pm) were selected to represent the chilled water system working under spring, mild-summer and sunny-summer days. The cooling load profiles of the three days are the measured data of the real building studied, as shown in Fig.6. The faults introduced in the simulation tests separately include AHU coils degradation (simulated by increasing thermal resistance of water side) and heat exchangers degradation (simulated by reducing heat transfer coefficient). During each test day, two severity levels of each fault were introduced separately in increasing order. 30 samples points under each fault level were selected in each test day. The residuals of the performance indices were calculated using the measured data and then compared with their thresholds. Fig.7-Fig.10 show the test results. In the figures, the solid points, "•", represent the residual values. The solid lines in the figures indicate the threshold band, which is calculated using Eq. (5) with 95% confidence. The points within the threshold band indicate that the corresponding performance indices are in

fault-free conditions. The points beyond the threshold band indicate that the corresponding performance indices are in the abnormal conditions.

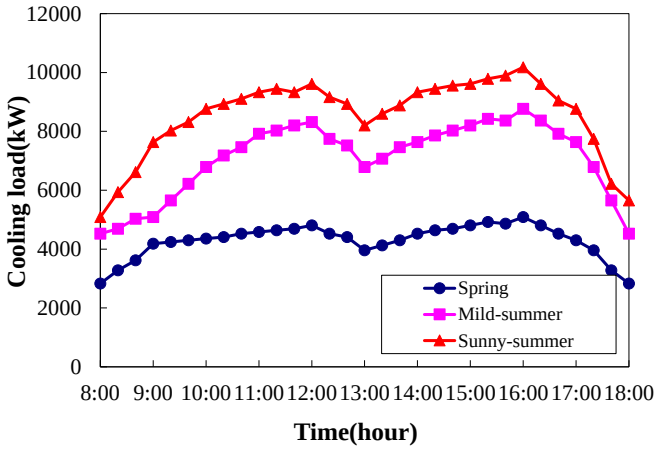

Fig.6 Cooling load profiles of three typical days

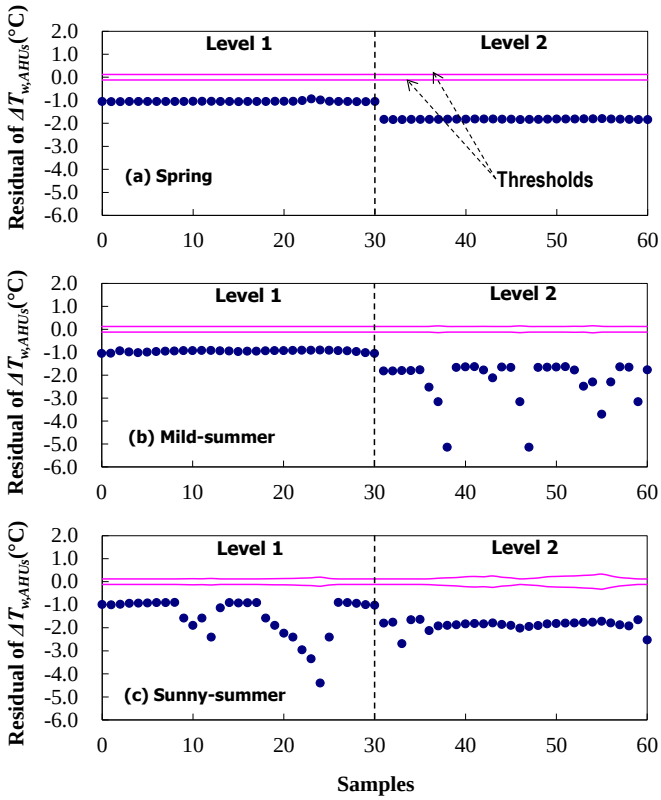

Fig.7 Residuals of $\Delta T_{w,AHUs}$ of global AHUs

Fig.7 and Fig. 8 show the residuals of performance indices and their thresholds in the global AHUs system when the water thermal resistance of cooling coils was increased by 40% (level 1) and 80% (level 2) respectively. The residual of $\Delta T_{w,AHUs}$ actually indicates the deviation of the measured system water temperature difference from the normal level. It can be observed

in Fig.7 that $\Delta T_{w,AHUs}$ is a very sensible performance index to the fault of coil performance degradation. In the three cases, all the points are located out of the threshold band, which means the water temperature difference ($\Delta T_{w,AHUs}$) is abnormal. The negative residual of $\Delta T_{w,AHUs}$ indicates the temperature difference produced by the overall AHUs is lower than the normal value and the system is suffering from the low delta-T syndrome. When the faulty severity level increases, larger deviations of the residuals occur. It is worth noticing that some points deviate more than 2°C from the threshold band in the mild-summer day (Level 2) and in the sunny-summer day (Level 1). The reason is that, under these operating conditions, the outlet air temperature of AHUs could not be maintained at the preset set-point due to the degraded heat transfer capacity of AHUs, which in turn resulted in more supplied chilled water and lower water temperature difference.

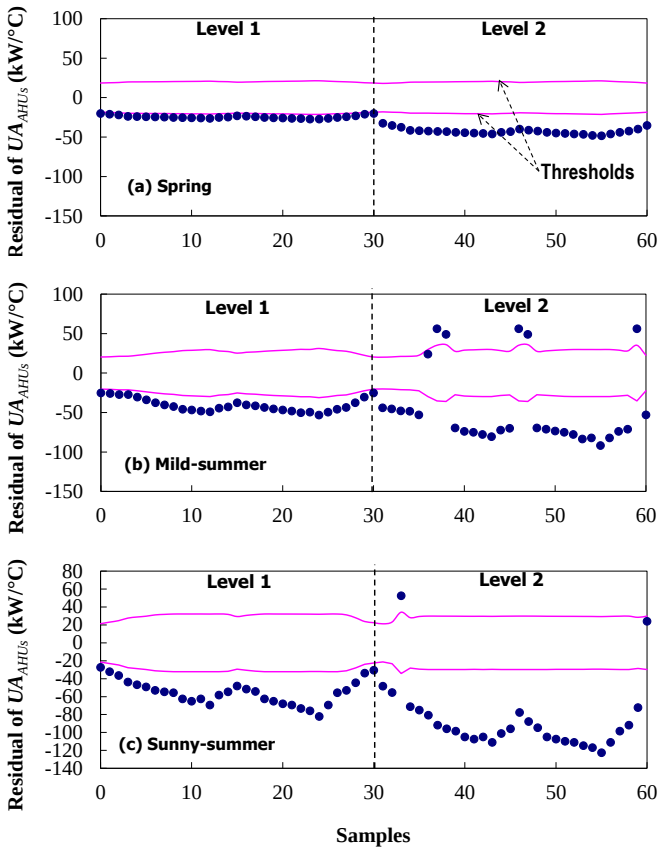

Fig.8 Residuals of UA_{AHUs} of global AHUs

Compared to the performance index of $\Delta T_{w,AHUs}$ of AHUs, the performance index of UA_{AHUs} are less sensitive to the detection of coil degradation. As shown in Fig.8, the residuals of UA_{AHUs} are very close to the thresholds under the faulty severity of Level 1 (particularly in

spring day) although the detection rate of UA is near 100%. When the faulty severity level is increased to Level 2, a larger deviation from the threshold can be observed.

The test results illustrate that the two performance indices ($\Delta T_{w,AHUs}$ and UA_{AHUs}) can be used as the indicators to diagnose the low delta-T syndrome of the AHUs system. It is noted that, when the two performance indices are abnormal simultaneously, it means the low delta-T syndrome occurs and the reduced coil effectiveness is just one of the contributors and not the exclusive one.

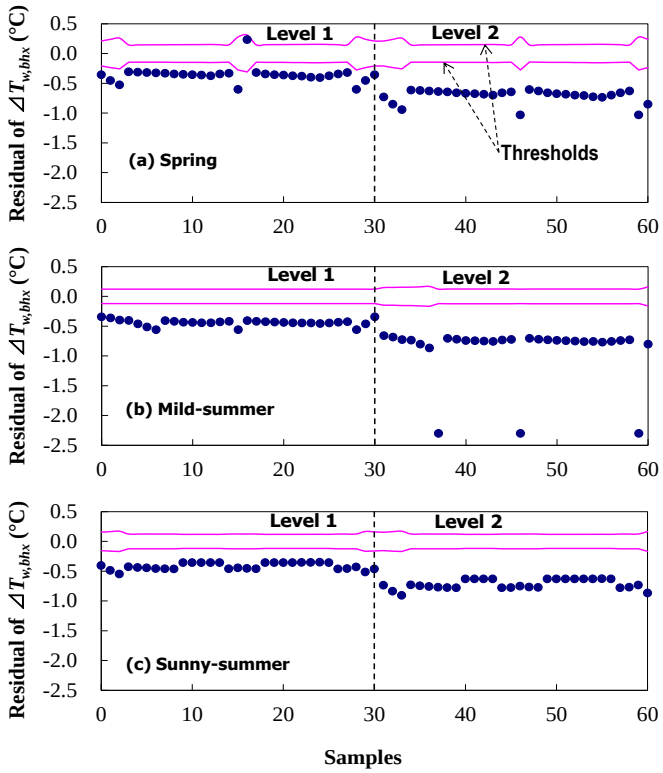

Fig.9 Residuals of ΔT_{bhx} of heat exchanger system

Fig.9 and Fig.10 show the residuals of two performance indices (i.e. ΔT_{bhx} (the overall water temperature difference at the primary side of heat exchanger group) and UA_{HX} (the overall conductance–area product of heat exchanger group) and their thresholds of the heat exchanger system when the heat transfer efficiency is decreased by 20% (level 1) and 30% (level 2) respectively. It is obvious that both ΔT_{bhx} and UA_{HX} are sensitive to the heat transfer efficiency degradation at two levels. ΔT_{bhx} residuals deviate obviously from the threshold band, which indicates that the water temperature difference at the primary side of the heat exchangers is lower than the normal value (i.e., low delta-T syndrome occurs). It is noted that

there are several points whose deviations are larger than 2°C in the test case of the mild-summer day in Fig.9. This is because that excessive water is delivered before heat exchanger group under these operating conditions due to that the outlet water temperature after heat exchangers could not be maintained at its set-point. When the supplied water to heat exchanger group is more than the water in the chiller loop, the deficit flow is triggered in the bypass line.

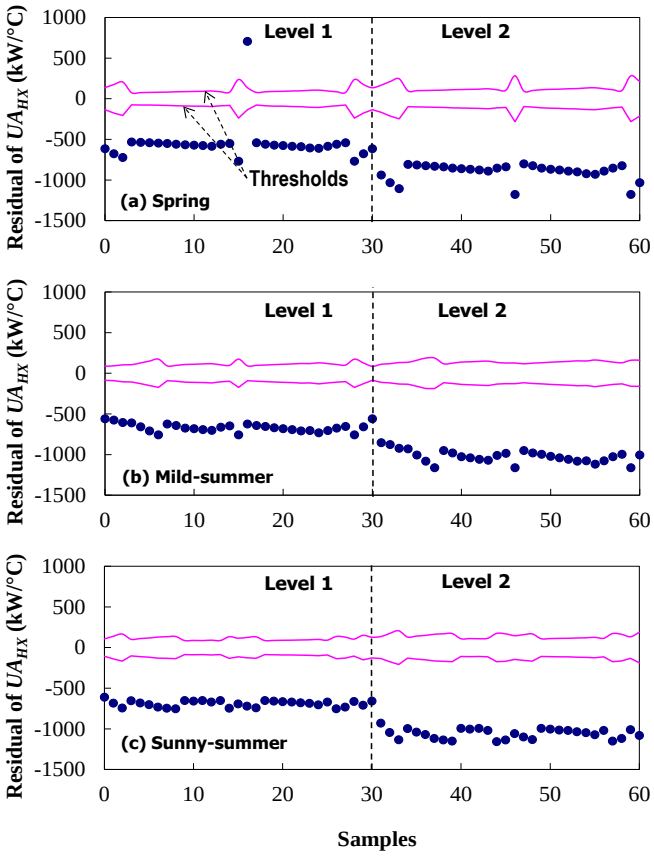

Fig.10 Residuals of UA_{HX} of heat exchanger system

The test results illustrate that the two performance indices (ΔT_{bhx} and UA_{HX}) can be used as the indicators to diagnose the low delta-T syndrome of at the primary side of heat exchanger group. It is noted that, when the two performance indices are abnormal simultaneously, it means the low delta-T syndrome occurs and the heat exchanger degradation is just one of the contributors. It could not prove that the low delta-T syndrome is totally caused by the heat exchanger degradation.

The detailed quantitative validation results are summarized in Table 4, where the detection

ratio of a performance index is a percentage of the point number outside of the threshold among the total point number. Obviously, most of the detection ratios of performance indices are near 100%, which means the faults can be successfully detected and diagnosed using the proposed FDD strategy under the faulty severity levels defined in this study.

Table 4 Summary of the detection ratios of proposed performance indices

Faults of Sub-systems	Performance indices	Spring		Mild-summer		Sunny-summer	
		Level 1	Level 2	Level 1	Level 2	Level 1	Level 2
AHU coils degradation	ΔT_{AHUs}	100%	100%	100%	100%	100%	100%
	UA_{AHUs}	100%	100%	100%	96.8%	100%	96.8%
Heat exchanger coils degradation	ΔT_{bhx}	96.8%	100%	100%	100%	100%	100%
	UA_{HX}	100%	100%	100%	100%	100%	100%

Using Eq. (10), the deviations of each performance index from the normal values can be calculated, in which the impacts of both the measurement uncertainty and the model fitting uncertainty are considered. Actually, the deviations of ΔT_{AHUs} and ΔT_{bhx} quantitatively evaluate the healthy status of the water temperature differences of the AHUs system and the heat exchangers group. Fig. 11 and Fig. 12, as examples, show the detailed deviations of related performance indices in the mild-summer case.

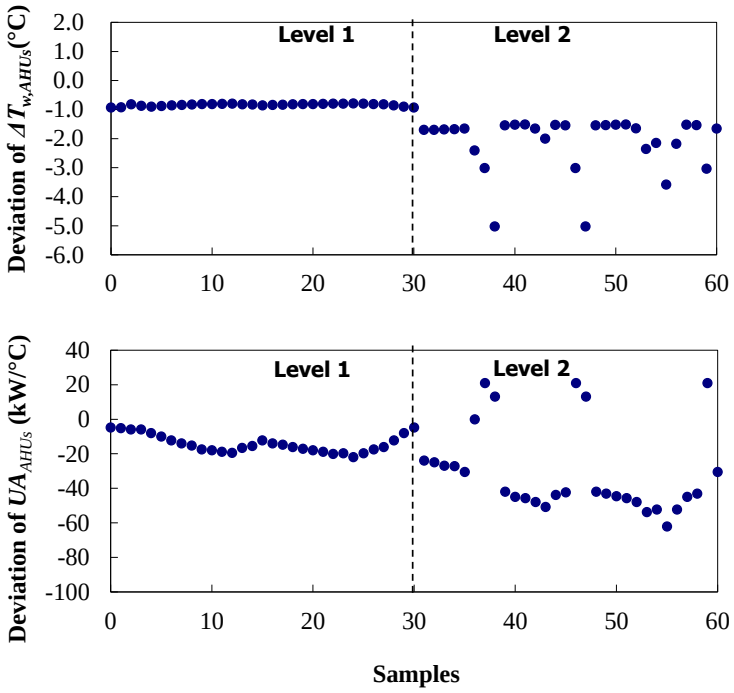

Fig.11 Deviations of performance index of AHUs (mild-summer case)

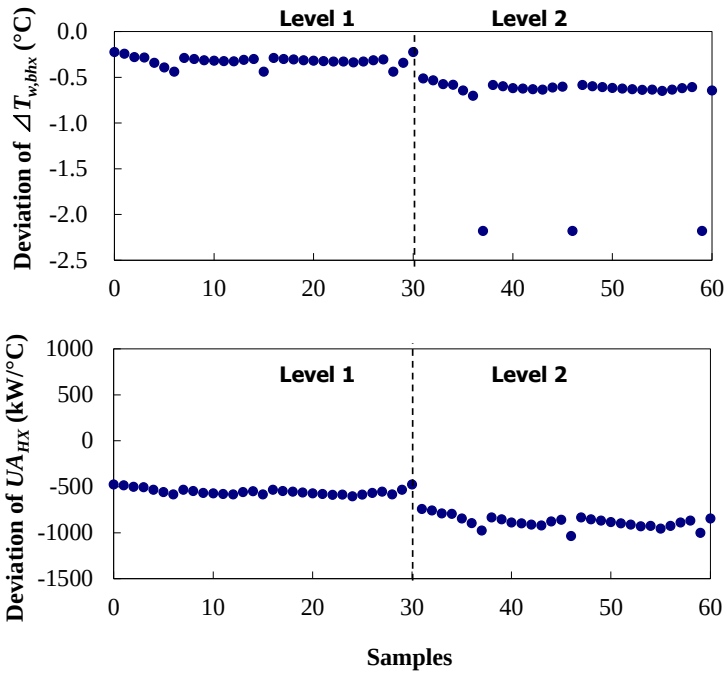

Fig.12 Deviations of performance index of heat exchanger group (mild-summer case)

5. Conclusion

A system-level fault diagnosis strategy for detecting and diagnosing the low delta-T syndrome was developed for the complex HVAC systems involving plate heat exchangers. Performance indices are developed to characterize the healthy status of the AHUs system and the plate heat exchanger system. Reference models and adaptive thresholds are adopted in the FDD strategy to detect and identify the faults. The proposed FDD strategy was validated in a dynamic simulation platform built based on a real complex HVAC system under three typical weather conditions.

It is found that the reference models have good performance in predicting the benchmarks of the corresponding performance indices. Particularly, the introduction of the load ratios of individual AHUs is proved to highly enhance the accuracy of the reference model for predicting the overall water temperature difference of the AHUs system. The results show that the proposed FDD strategy can detect and quantitatively evaluate the low delta-T syndrome. Two main causes of the low delta-T syndrome, performance degradations in the AHUs and the heat exchanger systems, are also can be identified successfully.

As far as the application issue is concerned, the system-level FDD method is easily applicable for practical applications due to the fact that it diagnoses the AHUs system and the plate heat exchanger system as a whole and less sensors are required when compared to

component-level method. Compared to the on-site observations based on the professional experiences, this FDD method can help the operators to detect the low delta-T syndrome and quantitatively assess the severity level. For the future works, the FDD method will be tested in the real HVAC system when significant fouling occurs in the system.

Acknowledgements

The research presented in this paper is financially supported by a grant (5276/12E) of the Research Grant Council (RGC) of the Hong Kong SAR and a grant of The Hong Kong Polytechnic University. The authors would like to acknowledge the support of Sun Hung Kai Real Properties Limited.

References

[1] U.S. Department of Energy. Building energy data book 2010; 2010.
[2] W. Kirsner. Demise of the primary-secondary pumping paradigm for chilled water plant design. HPAC Engineering, 1996; 68:73-78.
[3] J.P. Waltz. Variable flow chilled water or how I learned to love my VFD. Energy Engineering 2000; 97:5-32.
[4] W. Kirsner. Rectifying the primary-secondary paradigm for chilled water plant design to deal with low ΔT central plant syndrome. HPAC Engineering 1998;70:128-131.
[5] D.P. Fiorino. Achieving high chilled-water delta Ts. ASHRAE Journal 1999;41: 24–30.
[6] McQuay, Chiller Plant Design: Application Guide AG 31-003-1, McQuay International, 2002.
[7] S.T. Taylor, Degrading chilled water plant delta-T: causes and mitigation, ASHRAE Transaction 108 (1) (2002) 641–653.
[8] T.H. Durkin, Evolving design of chiller plants, ASHRAE Journal 47(11) (2005) 40–50.
[9] D.C. Gao, S.W. Wang, Y.J. Sun and F. Xiao. Diagnosis of the low temperature difference syndrome in the chilled water system of a super high-rise building: A case study. Applied Energy 2012; 98: 597–606
[10] D. P. Fiorino. How to Raise Chilled Water Temperature Differentials. ASHRAE Transactions 2002; 108: 659–665.
[11] G. Avery. Improving the efficiency of chilled water plants. ASHRAE Journal, 2001;43: 14–18.
[12] S.W. Wang, Z.J. Ma, D.C. Gao. Performance enhancement of a complex chilled water system using a check valve: Experimental validations. Applied Thermal Engineering 2010; 30: 2827–2832.
[13] Z.J. Ma, S.W. Wang. Enhancing the performance of large primary-secondary chilled water systems by using bypass check valve. Energy 2011; 36: 268–276.
[14] S.W. Wang, D.C. Gao, Y.J. Sun and F. Xiao. An online adaptive optimal control strategy for complex building chilled water systems involving intermediate heat exchangers. Applied Thermal Engineering 2013; 50: 614-628.
[15] D.C. Gao, S.W. Wang and Y.J. Sun. A fault-tolerant and energy efficient control strategy for primary–secondary chilled water systems in buildings, Energy and buildings 2011, 43(12): 3646–3656.
[16] Daniel A. Veronica. Detecting Cooling Coil Fouling Automatically—Part 1: A Novel Concept. HVAC&R Research 2010; 16(4): 413-433.
[17] Daniel A. Veronica. Detecting Cooling Coil Fouling Automatically—Part 2: Results Using a Multilayer Perceptron. HVAC&R Research 2010; 16(5): 599-615.
[18] Jonsson, G.R., S. Lalot, O.P. Palsson and Bernard Desmet. Use of extended Kalman filtering in

detecting fouling in heat exchangers. International Journal of Heat and Mass Transfer 2007; 50: 2643-2655.
[19] Ingimundardóttir H., & S. Lalot. Detection of fouling in a cross-flow heat exchanger using wavelets. International Conference on Heat exchanger Fouling and Cleaning, 2009.
[20] Z.J. Ma, S.W. Wang, and WK. Pau. Secondary loop chilled water in super high-rise. ASHRAE Journal 2008; 50: 42-52.
[21] Z.J. Ma, S.W. Wang. Supervisory and optimal control of central chiller plants using simplified adaptive models and genetic algorithm. Applied Energy 2011; 88: 198–211.
[22] Z.J. Ma, S.W. Wang .An optimal control strategy for complex building central chilled water systems for practical and real-time applications. Building and Environment 2009; 44: 1188–1198.
[23] J.T. Cui, S.W. Wang. A model-based online detection and diagnosis strategy for centrifugal chiller systems. International Journal of Thermal Sciences 2005; 44: 986-999.
[24] S.W. Wang. Dynamic simulation of a building central chilling system and evaluation of EMCS on-line control strategies. Building and Environment 1998; 33(1):1-20.